Journal of Pharmaceutical Innovation (2023) 18:1415–1426
https://doi.org/10.1007/s12247-023-09732-7

ORIGINAL ARTICLE

Development and Characterization of Soy Lecithin Liposome as Potential Drug Carrier Systems for Doxorubicin

Shaimaa A. Ahmed[1] · Aida A. Salama[1] · Mohamed H. Gaber[2] · Said A. Ali[2]

Accepted: 4 April 2023 / Published online: 9 May 2023

Abstract

Purpose The phospholipids from plant origins play an important role in different techniques, especially in drug delivery applications. The purpose of this study is to investigate the effect of liposomes prepared from plant origin as a cheap source of lipids as drug carriers.

Methods Soy lecithin liposomes (SLP) were prepared and loaded with doxorubicin (DOX) to use as a drug delivery system. DOX was used as the model drug and DOX/SLP was successfully combined. The characteristics of these liposomes, zeta potential, size distribution, drug encapsulation efficiency (EE%), drug release, Fourier transform infrared (FTIR), and transmission electron microscopy (TEM) were checked followed by in vitro study. The cytotoxicity study by using free DOX and DOX/SLP is done on Mcf-7, human breast cancer as a cell line.

Results The optimal DOX/SLP formulation had a mean size of 342 nm, a negative zeta potential of −22.3 mV, the loaded DOX/SLP showed EE% (83.68%), and a drug release profile of 35 h, all are recorded. Cytotoxicity assay showed that the IC_{50} of DOX/SLP is smaller than that of free DOX.

Conclusion These results give evidence of the efficacy of using drug carriers from plant origin combined with drugs to increase the effective therapies against cancer medically and economically.

Keywords Drug delivery · Drug carriers · Doxorubicin · Soya lecithin · Liposomes

Abbreviations

Conc.	Concentration
DLE	Drug loading efficiency
DOX	Doxorubicin
DOX/SLP	Doxorubicin/soy lecithin liposome
EE%	Encapsulation efficiency
FTIR	Fourier transform infrared
TEM	Transmission electron microscopy
PA	Phosphatidic acid
PBS	Phosphate buffer solution
PC	Phosphatidylcholine
PE	Phosphatidyl-ethanolamine
PI	Phosphatidyl-inositol
Rpm	Revolution per minute
SL	Soy lecithin
SLP	Soy lecithin liposome
Tm	Transition temperature

✉ Said A. Ali
saidataha@cu.edu.eg

Shaimaa A. Ahmed
Shaimaaabdellateif.5919@azhar.edu.eg

Aida A. Salama
Salama.aida@yahoo.com

Mohamed H. Gaber
Gaberm@sci.cu.edu.eg

[1] Biophysics branch, Physics Department, Faculty of Science (Girls branch), Al-Azhar, University, Cairo, Egypt

[2] Biophysics Department, Faculty of Science, Cairo University, Giza, Egypt

Introduction

Liposomes are vesicles formed from non-toxic surfactants, cholesterols, glycolipids, sphingolipids, long-chain fatty acids, and even membrane proteins. When phospholipids are dissolved in water, they form a closed structure with an internal aqueous environment bounded by phospholipids bi-layer membranes, this vesicular system is called liposome [1]. Phospholipids from soy lecithin are vastly used in liposomal drug delivery because they can include in their internal compartment water in which hydrophilic components can be dissolved while lipophilic drugs can be

entrapped within the space between the lipid's layers [2]. Liposomes improve therapeutic efficacy by promoting drug absorption while avoiding fast degradation and side effects, extending the biological half-life, and reducing toxicity [3]. The unique advantage of liposomes is that they are biocompatible, biodegradable lipids, inert, and non-immunogenic. Liposomes can be used to entrap hydrophilic compounds in the inner core and/or lipophilic molecules in the double lipidic layer [4].

Soybean is the main phospholipids in plants. Lecithin from soybean is a complex mixture containing phosphatidylcholine (PC), phosphatidic acid (PA), phosphatidylethanolamine (PE), phosphatidylinositol (PI), triglycerides, sphingolipids, glycolipids, and free fatty acids [5]. Lecithin from soybeans is highly preferable for pharmaceutical industries application due to its emulsifying properties, non-antigenic nature, safe, wide availability, and low cost for production [6].

Chemotherapy plays a major part in cancer treatment, especially breast cancer, lung cancer, lymphoma, thyroid cancer, cervix cancer, etc. There are different types of chemotherapy each with distinct late effects. Some of the late side effects are second malignancy, pulmonary complications, psychosocial difficulties, and cardiac toxicity [7].

Doxorubicin (DOX) is an antibiotic drug derived from the streptomyces paucities bacterium. It is a part of the anthracycline group of chemotherapeutic agents [8]. The mechanism of actions of DOX, in cancer cells, are as follows: (i) interpolation into DNA and disruption of topoisomerase II-mediated DNA and (ii) generation of free radicals which damage cellular membranes, causing DNA strands breakage and inhibition of both DNA and RNA synthesis [9]. Briefly, DOX is oxidized, an unstable metabolite, which releases reactive oxygen species. These species lead to lipid peroxidation and membrane damage, DNA damage, oxidative stress, and trigger apoptotic pathways of cell death [10]. In this study, doxorubicin/soy lecithin liposomes (DOX/SLP) were prepared through two steps that included the preparation of liposomal thin film from soy lecithin and conjugated with doxorubicin. This study aims to create an SLP system for the effective delivery of DOX, to tumor cells by increasing the half-life circulation of DOX/SLP. SLP was synthesized by using the thin film hydration method and then mixed with DOX. The obtained particles from DOX/SLP were reduced in size distribution by sonication. The physical and chemical properties of liposomal formulations were characterized by Fourier transform infrared (FTIR), size distribution, zeta potential measurement, transmission electron microscopy (TEM), drug release, encapsulation efficiency, and fluorescence measurements determined.

Materials

Soy lecithin (SL) powder ($C_{35}H_{66}NO_7P$) was purchased from bulksupplements.com, 7511 Eastgate Rd, Henderson, NV 89,011, the USA, with a molecular weight of 643.87 g/mol. Cholesterol (CHOL) $C_{27}H_{46}O$ with MW: 386.65 gm/mol, with melting point 148–150 °C was purchased from ADVENT CHEMBIO PVT LTD. Adricin, doxorubicin HCL ($C_{27}H_{29}NO_{11}$) solution 50 mg/25 ml (DOX) manufactured by Hikma Specialized Pharmaceuticals, Badr City, Cairo, A.R.E, with molecular weight 543.52 g/mol. Chloroform (trichloro methane) $CHCl_3$ contains 0.8% ethanol as a stabilizer, with assay ≥ 99.5%, molecular weight 119 g/mol, ethanol (EtOH) C_2H_5OH with concentration 99%, melting point −114.1 °C, molar mass 46.07 g/mol, and sodium chloride as saline (NaCl, with pH 5.5) 0.9%. The dialysis bag was made from regenerated cellulose (RC) with glycerol as a protector from embrittlement. It is suitable for a pH range of 2–12 and a temperature of 4–60 °C with a diameter of 21 mm and 5 m in length with a molecular weight cutoff of 5 KDa (about 5 cm of the dialysis tubing bag used in our experiment).

Methods

Liposomal Preparation and Drug Loading

Two samples of SLPs were prepared by the thin-film hydration method. One was used as a blank while the second was loaded with DOX. Alternatively, in blank, a weighed SL powder of about 1.01 mol is dissolved in chloroform and sonicated with saline (0.9%) for 60 min at least, while in DOX/SLP, accurately weighed SL powder, cholesterol, and DOX, at a ratio of 9:1:0.5 (wt/wt/wt). Firstly, SL and cholesterol were dissolved in chloroform in a round-bottom flask, using a rotary evaporator to evaporate all chloroform and to obtain a thin film under vacuum at a maximum of 50 °C and maintained under vacuum conditions overnight to remove all traces of the solvent. The lipid film was hydrated with DOX (in liquid form) which was dispersed by sonication for 60 min. Finally, both the obtained SLP and DOX/SLP dispersion were stored at 3–7 °C.

Molecular Structure Characterization

The chemical structures of all samples were analyzed by FT/IR spectroscopy (4600 type A; National Research Center, Cairo, Egypt). KBr sandwiches were pellet perfectly and all samples were prepared by mixing with them separately. Spectra were acquired in the range of 4000 to 400 cm^{-1} with

a resolution of 4 cm^{-1}. Background scans were acquired and then subtracted from the spectrum of the sample.

Standard Curve for Doxorubicin

Each vial of adricin (25 ml) contains doxorubicin HCl 50 mg. Therefore, the total vial concentration is 50 mg/25 ml which means 2 mg/ml. Different concentrations of DOX are prepared, and its absorbance is measured using the fluorimeter technique at the wavelength (excitation) of 470 nm. The standard curve of DOX is made as a relation between concentration on *X*-axis and absorbance on *Y*-axis.

Drug Loading Efficiency

Substantially, 1 ml DOX/SLP was diluted in 6 ml phosphate-buffer solution (PBS, with pH = 7.2) by using ultracentrifugation at 12,000 rpm for 15 min at 4 °C to separate free DOX as a supernatant, from encapsulated one. Then take 0.1 ml from the supernatant and diluted it with 0.9 ml of NaCl saline. The absorbance of the supernatant which contains the free DOX is measured using fluorimeter apparatus. From the DOX standard curve, the corresponding concentration is measured. By using the solution dilution calculator to determine the residual concentration ($C_1V_1 = C_2V_2$), then the DOX loading efficiency (DLE) of DOX/SLP is calculated using Eq. (1) [11]:

$$DLE\ (\%) = \frac{(Total\ drug - free\ drug)}{Total\ drug} \times 100 \quad (1)$$

Drug Release

A dialysis bag is a tube made from regenerated cellulose (RC) with glycerol as a protector from embrittlement which can be easily removed by soaking in water. In our research, about 5 cm of the dialysis tubing bag was used in the experiment. The tube was washed in distilled water several times and filled with 2 ml from our sample (DOX/SLP), closed up and down with clips, and then placed in a beaker containing 30 ml of NaCl saline or until the was bag covered with saline. The beaker was placed on low stirring all time of the experiment at room temperature. Samples were taken after 2, 4, 6, 24, and 35 h. After each sample, the same quantity of fresh saline is added. The corresponding absorbance is measured for each sample using fluorimeter fluorescence apparatus. Finally, the drug release curve is plotted between the time and absorbance.

Determination Size and Zeta Potential

The particle size and zeta potential of SLP and DOX/SLP were determined by a dynamic light scattering (DLS) Zetasizer Nanoseries (Malvern Instruments, UK) analyzer which provides information on particle size, zeta potential, concentration, and molecular weight. The samples were diluted 100 times before measurements. Set the detection angle at 90° and the temp. of 25 °C and the refractive index. Using a Helium–Neon LASER beam, choose the suitable cuvette for the sample then start the analysis.

Transmission Electron Microscopy (TEM)

A JEM-2100 HR TEM [(200 kV; JEOL, Japan); National Research Center, Cairo, Egypt] was used to observe the morphology of the prepared samples, SLP and DOX/SLP. The samples were prepared by placing a drop of phosphortungsten acid (transmittance negative stain) on carbon-coated copper and left to air-dry before imaging.

In Vitro Cell Line Study

The cytotoxicity assay was administered in a human breast cancer cell line (Mcf-7) for both DOX and DOX/SLP samples. Mcf-7 cells were seeded at a density of the order of 1×10^5 cells/ml (100 µl/well) that was dispensed during a 96-well tissue culture plate and incubated at 37 °C for 24 h to develop a complete monolayer sheet. The two-fold dilutions of tested samples were made in RPMI medium with 2% serum. A total of 0.1 ml of every dilution was tested in different wells leaving 3 wells as control receiving only maintenance medium. The plate was incubated at 37 °C and examined. MTT solution was prepared (5 mg/ml in PBS). Twenty microliters of MTT solution was added to every well and placed on a shaking table (150 rpm for 5 min) to mix MTT with media. Incubate (37 °C, 5% CO_2) for 4 h to permit the MTT to be metabolized. Dry the plate on paper towels to get rid of residue if necessary. Re-suspend formazan (MTT metabolic product) in 200 µl DMSO, and place it on a shaking table (150 rpm for 5 min). Read the optical density at 560 nm and subtract the background at 620 nm [12].

Statistical Analysis of Data

All data were expressed as mean ± SD. The statistical analysis was performed using Excel 2010, origin 2018, and ANOVA with $p < 0.05$ to consider all data statistically significant.

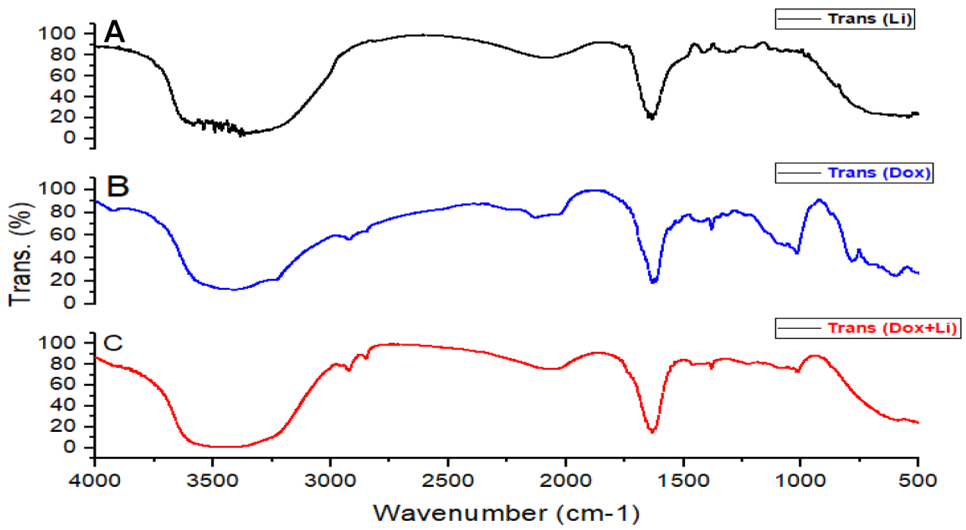

Fig. 1 The Fourier transform infrared (FTIR) spectra of SLP (**a**), Dox (**B**), and DOX./SLP (**C**)

Results and Discussion

Synthesis and Characterizations of SLP and DOX/SLP

The primary characterization of SLP, DOX and DOX/SLP was performed through FTIR spectra as shown in (Fig. 1A–C), respectively. Band area values were calculated using a linear baseline from 4000 to 2500 cm^{-1}, from 2500 to 1500 cm^{-1}, and the fingerprint from 1500 to 300 cm^{-1}.

As shown in the spectrum of SLP, the absorption band 2079 cm^{-1} (N = C = S), 1762 cm^{-1} (Cl–C = O), 1640 cm^{-1} (C = C), 1321 cm^{-1} (COO-), 1247–1206 cm^{-1} (C-O), 1112 cm^{-1} (CO–O-C), and 849 cm^{-1} (C–Cl) are identified. The spectrum was similar to DOX/SLP spectrum except for the appearance of bands at 3432 cm^{-1} (O–H), 3000–2850 cm^{-1} and at 1457–1383 cm^{-1} (C-H), 1086 cm^{-1} (C-F), 1018 cm^{-1} (C-N) (amine), and at 593 cm^{-1} (C–Br) [13]. Note also that the sharp peak in SLP that corresponds to the C = O disappeared in DOX/SLP, because of the presence of cholesterol chloroformate in the sample; the band Cl–C = O disappeared which means that DOX is successfully conjugated with SLP [14]. The shift of the C = C bond means there is a decrease in the frequency that marks the formation of new hydrogen bonds between components [15].

Standard Curve and Drug Loading Efficiency of DOX

For constructing the standard curve, 1 ml of DOX was diluted to different concentrations (Conc.). The absorbance of each concentration is measured by a fluorimeter. The absorbance of each sample is measured at a wavelength of 470 nm (excitation) which is plotted as a function of DOX concentration as shown in (Fig. 2). This curve will be used to calculate the drug loading efficiency (DLE) of DOX. To calculate the DLE of DOX, 1 ml of DOX/SLP was diluted in 6 ml of PBS with pH = 7.2 and then centrifuged at 12,000 rpm for 15 min at 4 °C.

Then, separate the supernatant which contains the free DOX, from that bound with SLP. A total of 0.1 ml of supernatant is diluted with 0.9 ml of PBS buffer solution, and use fluorimeter to get its absorbance. By using the standard curve, the corresponding diluted Conc. (0.03265 mg/ml) is determined from the measured absorbance value and using Eq. (2). Thus, the encapsulated drug is calculated to be 1.673 mg/ml.

$$C_1V_1 = C_2V_2 \tag{2}$$

The total vial Conc. is 2 mg/ml. So, the encapsulated drug is calculated to be 1.673 mg/ml. From Eq. (1), The DLE% is calculated to be 83.68%. That tells us that larger particles size has large cores, which allow more drugs to be encapsulated per particle and give slower release. Thus, as we

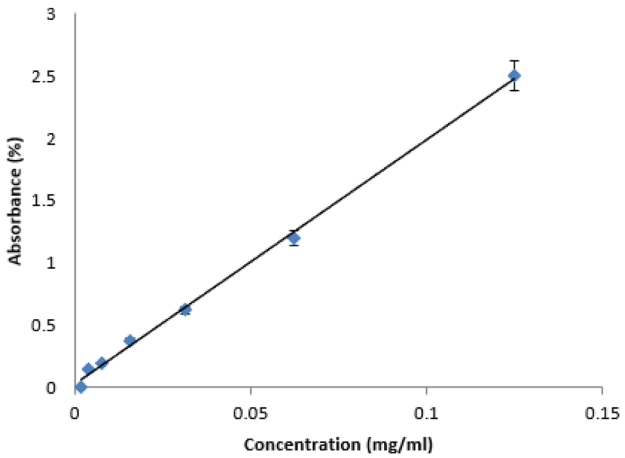

Fig. 2 Standard curve of doxorubicin

control particle size, it provides a means of regulating drug release rates and increasing encapsulation efficiency [16]. Also, DOX is positively charged because of its protonatable amino group, so it can engage in electrostatic interactions with full or partially negatively charged groups in the SLP [17]. This all leads to increasing the EE%.

Determination of Phase Transition Temperature (T_m)

The phase transition of DOX/SLP was determined using an RF-5301PC Spectro fluorophotometer connecting with a water bath equipped with a thermocouple. This device is an important tool for the trace analysis of compounds that have functional groups that exhibit fluorescence. In this technique, the sample was diluted (0.1 ml of sample: 1.5 ml of saline), and then put the sample in the cuvette chamber which is connected to the water bath circulator. Starting from 25 to 65 °C, the intensity of fluorescence reading is recorded every 2 °C. The recorded fluorescence values are plotted as a function of temperature as shown in (Fig. 3).

As shown in (Fig. 3), the T_m of DOX/SLP is calculated. It is found that in DOX/SLP, the T_m increased to 47.4 °C in comparison with SLP as blank (O'Neil SD, 1982) [18]. This increase in T_m because of cholesterol in the lipid led to a decrease in the fluidity of the membrane and gives stability to liposomes and a decrease of uptake by the Reticulo-endothelial-system [19].

Drug Release by the Dialysis Bag

In the beaker, put 30 ml of NaCl saline (pH 5.5) as a buffer, and 5 cm of dialysis bag filled with 2 ml of our sample DOX/SLP. Close the bag up and down with clips and then place it over low stirring all time during the experiment. The samples were taken every 2, 4, 6, 24, and 35 h, and their absorbance at a wavelength of 470 nm is measured using the fluorimeter device. The plotted curve is the time (hours) on the *X*-axis and release (%) the on *Y*-axis to get the release curve of DOX, as shown in (Fig. 4).

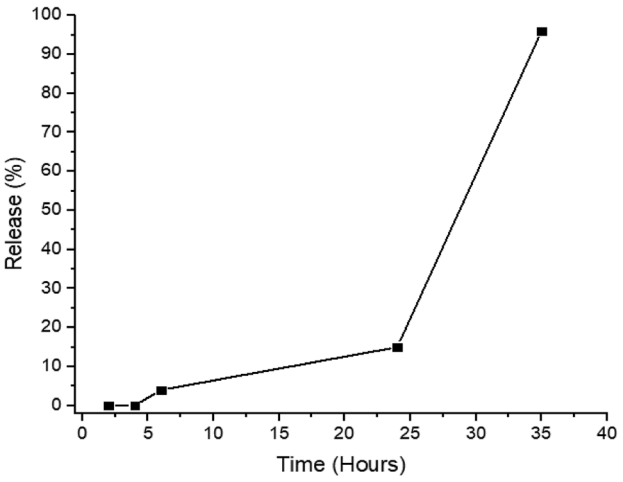

Fig. 4 Release profile of DOX, by dialysis bag

Drug release from DOX/SLP was very slow until 6 h and continued to increase until the end of the experiment. By using the standard curve in the analysis, it is found that after 6 h, only 4% of the total DOX Conc. in the bag was released, while after 24 h, about 15% of the total DOX Conc. in the bag was released. Until 35 h, about 96% of the total DOX concentration in the bag was released. In other words, the release behavior of DOX from loaded SLP was significantly slower than that of DOX alone. The result showed that doxorubicin release increased and then

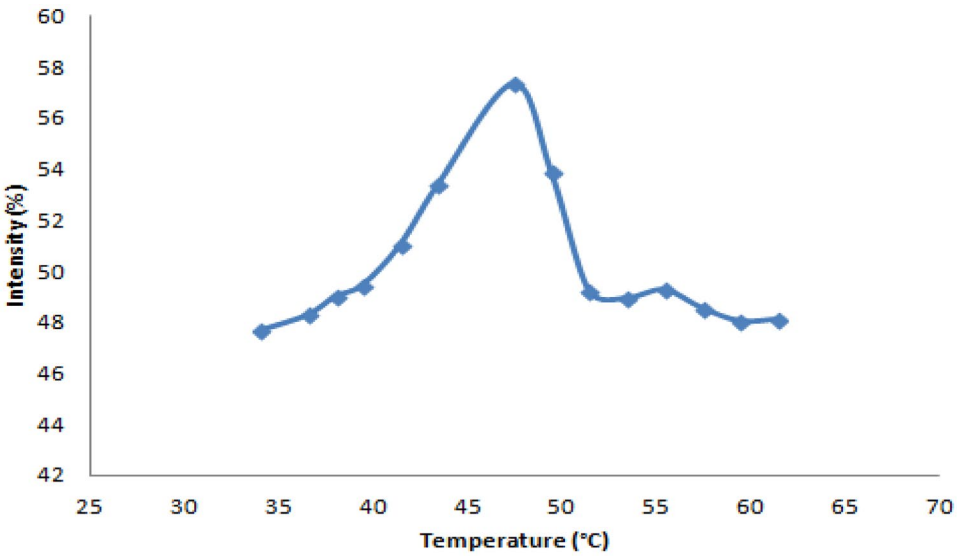

Fig. 3 Transition temp., of DOX/SLP

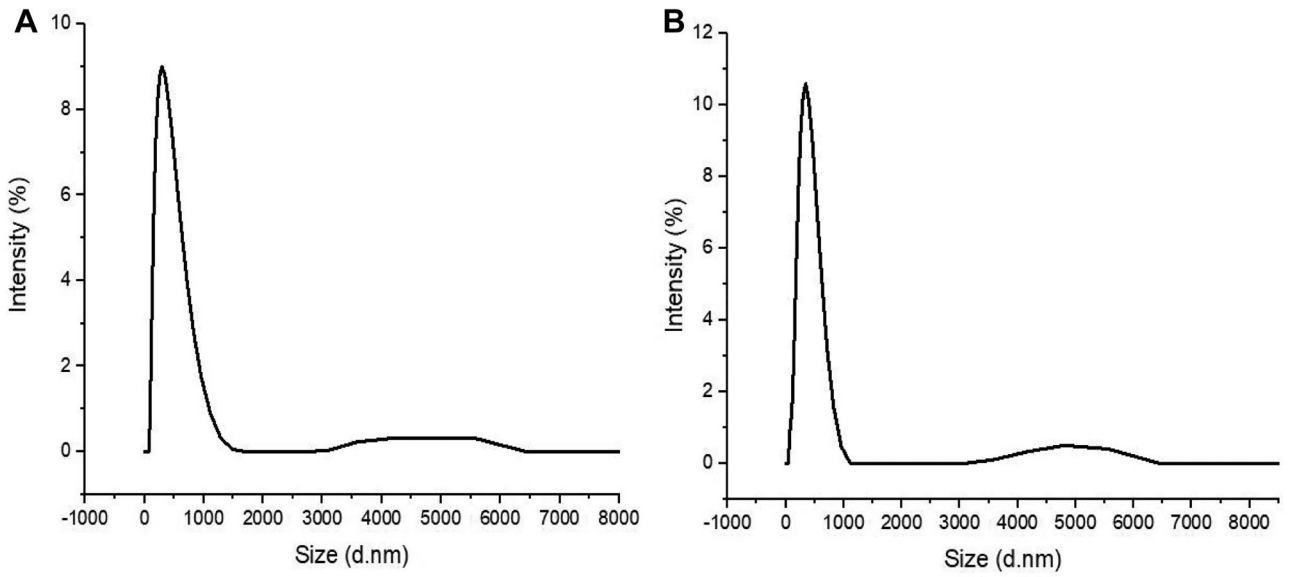

Fig. 5 DLS image size, of SLP (**A**) and DOX/SLP (**B**)

reached a plateau region after 6 h and remained mostly constant until 24 h, and then start to increase again. This suggested the release of Dox. from SLP is too low because Dox. inside the SLP present as a precipitate that supports the Dox. stability inside the SLP [20]. This release time increase helps to keep DOX/SLP in circulation for a longer time with min. amount of release in blood circulation. That helps in decreasing the side effects of DOX, as a drug on healthy tissue [21]. As the encapsulation efficiency is high, the stability of liposomes is high (size distribution, suitable preparation methods, usage of high-quality lipids, suitable preparation method, and storage conditions), all of this preventing drug leakage [22].

The Optimal Formulation of SLP and DOX/SLP

The size and zeta potential of SLP was measured to be 282 nm and −26.9 mV respectively, while the measured values of DOX/SLP were 342 nm and −22.3 mV respectively. As shown in (Fig. 5), there is an increase in size that can be explained by increasing the attractive force between SLP and DOX leading to increasing the size [23]. That size affects the amount of drug loading, which pivotally determines the pharmacokinetics and pharmacodynamics of the drugs in circulation [24]. As we know that zeta potential is the total surface charge and the stability of SLP or SLP/DOX. When liposomes have charge means, repulsive forces increase and the medium becomes stable. Zeta potential lesser than −30 mV or greater than 30 mV is considered to be more stable [25]. So, the magnitude of the zeta potential increase from −26.9 to −22.3 mV gives a sign of the potential stability of the sample, by increasing the repulsion between particles. This zeta potential has the possibility to improve biological performance by circumventing surface charge-related toxicities [26].

Transmit Electronic Microscope (TEM)

The morphology of both samples in detail was further confirmed by TEM. This technique can give highlight structural changes in any material. The samples were prepared by placing a drop from each sample on carbon-coated copper placed on filter paper. Let dry for a few seconds, then place a drop of transmittance-negative stain on it, and leave it to air-dry before imaging. As shown in (Fig. 6), TEM verified the presence of liposomes in round shape with multi-lamellar, 200 nm in width in the SLP sample while in DOX/SLP, the sample was round, dark in color because of DOX, and has around 320 nm in width. The TEM images showed that both SLP and DOX/SLP were spherical in morphology, and the liposomal system possessed a size range that fell into the therapeutic-potential range [27].

Cell Line Cytotoxicity

Cytotoxicity assays were performed to evaluate the biocompatibility of synthesized DOX/SLP as drug delivery systems in the normal cell line (Vero) (Table 1) and the human breast cancer cell line Mcf-7 in both low and high DOX and DOX/SLP concentrations (Tables 2 and 3) respectively, followed by Fig. 7 which describes the histograms ± SD of all analyses of cell viability. Results were expressed as the percentage of cell

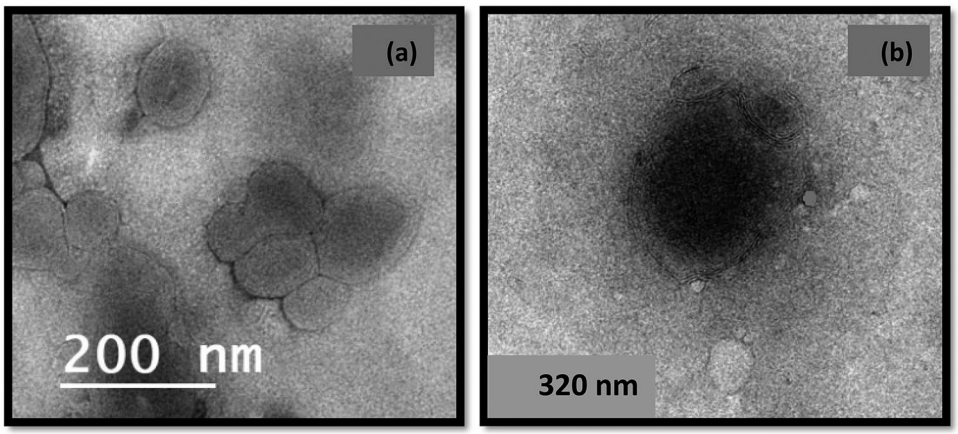

Fig. 6 TEM images, of SLP (**a**) and DOX/SLP (**b**)

proliferation, compared with 0.1% DMSO control and were calculated from Eq. (3) as follows [28]:

$$Viability\ (\%) = \frac{mean\ OD\ treated}{mean\ OD\ blank} \times 100 \quad (3)$$

As shown in (Table 1, Fig. 7A), the normal Vero cell line was exposed to 100, 50, 25, 12.5, 6.25, and 3.125 µg/ml of both DOX and DOX/SLP separately. When comparing cell viability at all conc. of DOX/SLP to cell viability of DOX only, a difference in cell viability was observed and cell viability decreased from low to high conc. in DOX/SLP records, while there is approximate stability of cell viability in lower conc. in DOX results. $IC_{50} \pm SD$ of both DOX and DOX/SLP was 41.75 ± 0.77 and 11.08 ± 0.07, respectively. This difference possibly returns to the mechanism of release of DOX from SLP over the incubation time [29].

As shown in (Table 2, Fig. 7B), cell viability assay can determine the effect of drug candidates on cells and be used to optimize the cell culture conditions. As shown DOX/SLP has an inhibition effect on cell growth [30]. This data represent the effect of DOX and DOX/SLP on Mcf-7 cell lines by using low sample conc. 100, 50, 25, 12.5, 6.25, and 3.125 µg/ml. These data showed that the conc. of the drug that needs to kill 50% of cancer cells is low in DOX/SLP rather than DOX only. When DOX/SLP reach the tumor site, they released DOX which is capable of diffusing through the tumor cell membrane to the nucleus which contains DNA of the tumor cell to block topoisomerase II and cause cell death [31]. $IC_{50} \pm SD$ of both DOX and DOX/SLP was 6.01 ± 0.28 and 4.81 ± 0.07. This indicates that liposomes form a shell around DOX, which led to reduced DOX release as indicated in the drug release profile described above, and the amount of DOX released increases after 72 h of injection [32].

The last one is shown in (Table 3, Fig. 7C), the effect of higher sample conc. 250, 125, 62.5, 31.25, 15.62, 7.81 µg/ml on Mcf-7 cell line. The same effect of DOX/SLP in higher conc. on higher conc. especially at 31.25, 15.62, and 7.81 µg/ml, is clearly shown a great difference in cell viability rather than DOX only. When DOX/SLP reaches the nuclease, a large amount of DOX diffuses into the tumors' nucleus. Overall

Table 1 Chemo-sensitivity testing in a normal cell line (Vero) using MTT assay (by single-fold dimension). This table shows the results were expressed as IC_{50}, i.e., the concentration of cytotoxic drug that reduces cell viability by 50% relative to the control

ID	µg/ml	O.D			Mean O.D	±SE	Viability %	Toxicity %	$IC_{50} \pm SD$
Vero	——	0.75	0.76	0.76	0.76	0.00	100.00	0.00	
DOX	100.00	0.07	0.11	0.09	0.09	0.01	12.21	87.79	41.75 ± 0.77
	50.00	0.25	0.28	0.27	0.26	0.01	34.92	65.08	
	25.00	0.60	0.62	0.63	0.62	0.01	81.75	18.25	
	12.50	0.74	0.75	0.76	0.75	0.00	98.94	1.06	
	6.25	0.75	0.76	0.75	0.75	0.00	99.65	0.35	
	3.13	0.75	0.75	0.76	0.76	0.00	100.00	0.00	
DOX + SLP	100.00	0.05	0.04	0.06	0.05	0.01	6.39	93.61	11.98 ± 0.07
	50.00	0.09	0.11	0.10	0.10	0.01	13.54	86.46	
	25.00	0.19	0.24	0.23	0.22	0.01	29.23	70.77	
	12.50	0.35	0.35	0.35	0.35	0.00	46.34	53.66	
	6.25	0.64	0.67	0.65	0.65	0.01	86.33	13.67	
	3.13	0.76	0.75	0.76	0.75	0.00	99.74	0.26	

Table 2 Chemo-sensitivity testing in Mcf-7 cell lines (low concentration) using MTT assay (by double-fold dimension). This table shows the results were expressed as IC50, i.e., the concentration of cytotoxic drug that reduces cell viability by 50% relative to the control

ID	µg/ml	O.D			Mean O.D	± SE	Viability %	Toxicity %	IC_{50} ± SD
Mcf7	——	0.63	0.65	0.65	0.64	0.01	100.00	0.00	µg
DOX	100.00	0.03	0.03	0.02	0.03	0.00	4.14	95.86	6.01 ± 0.28
	50.00	0.05	0.05	0.05	0.05	0.00	7.61	92.39	
	25.00	0.12	0.11	0.13	0.12	0.00	18.27	81.73	
	12.50	0.21	0.20	0.20	0.20	0.00	31.78	68.22	
	6.25	0.33	0.30	0.27	0.30	0.02	46.43	53.57	
	3.13	0.60	0.57	0.58	0.58	0.01	90.73	9.27	
DOX + SLP	100.00	0.02	0.02	0.02	0.02	0.00	2.80	97.20	4.81 ± 0.07
	50.00	0.04	0.04	0.03	0.04	0.00	5.85	94.15	
	25.00	0.12	0.11	0.12	0.12	0.01	17.96	82.04	
	12.50	0.14	0.17	0.15	0.15	0.01	23.91	76.09	
	6.25	0.23	0.27	0.25	0.25	0.01	38.82	61.18	
	3.13	0.40	0.39	0.42	0.41	0.01	62.94	37.06	

conc. IC_{50} ± SD of DOX. and DOX/SLP was 41.02 ± 0.66 and 27.72 ± 0.96, respectively. This proves that the encapsulation of DOX is high and SLP controlled in DOX release. So, it can be concluded that DOX/SLP are biocompatible, bioavailable, and appropriate for drug delivery systems [33].

The cell toxicity caused due to the action of a chemotherapeutic agent on Mcf-7 cells is described in After Analysis; it is clearly shown that at higher concentrations (250, 125, and 62.5 µg/ml), there is a low sample toxicity effect rather than free DOX. The smaller value of IC_{50} of DOX/SLP in all conc. means that the amount of drug-loaded liposome that needs to kill 50% of cancer cells is less than the amount of free drug, which concludes that much lower concentrations of drug load by liposomes will have as a great effect on cells as higher concentrations of free drugs which will greatly reduce the side effects of using larger doses of chemotherapeutic drugs [34].

There are some images that indicate the morphological changes on different cell lines, represented as follows: control cell line, after adding free DOX and after adding the same conc. from DOX/SLP. As shown in Figs. 8, 9, and 10, there is a clear difference between the effect of free DOX and DOX/SLP on the cancer cells.

According to published data in 2013, by comparing the therapeutic efficacy of Doxil (commercial doxorubicin-loaded-liposomes) prepared from animal origin source, the cytotoxicity as presented by its IC_{50} of free DOX, DOX/SLP, and Doxil is shown in (Fig. 11). The IC_{50} values of DOX, DOX/SLP, and Doxil are calculated to be 41.02 ± 0.66 µg/ml, 27.72 ± 0.96 µg/ml, and 32.2 ± 3.6 µg/ml respectively [35]. The smaller value of IC_{50} of DOX/SLP against free DOX and Doxil indicates the more therapeutic efficiency of DOX/SLP as a potential and novel chemotherapeutic confirmation concerning other chemotherapeutic drugs, such as free DOX and Doxil.

Table 3 Chemo-sensitivity testing in Mcf-7 cell lines (high concentration) using MTT assay (by double-fold dimension). This table shows the results were expressed as IC_{50}, i.e., the concentration of cytotoxic drug that reduces cell viability by 50% relative to the control

ID	µg/ml	O.D			Mean O.D	± SE	Viability %	Toxicity %	IC_{50} ± SD
Mcf7	——	0.88	0.90	0.87	0.88	0.01	100.00	0.00	Ug
DOX	250.00	0.02	0.03	0.03	0.02	0.00	2.80	97.20	41.02 ± 0.66
	125.00	0.08	0.09	0.07	0.08	0.01	8.69	91.31	
	62.50	0.20	0.19	0.22	0.20	0.01	22.75	77.25	
	31.25	0.49	0.47	0.47	0.48	0.01	53.85	46.15	
	15.62	0.84	0.89	0.86	0.86	0.01	97.81	2.19	
	7.81	0.87	0.89	0.88	0.88	0.00	99.58	0.42	
DOX + SLP	250.00	0.07	0.06	0.07	0.07	0.00	7.52	92.48	27.72 ± 0.96
	125.00	0.11	0.13	0.15	0.13	0.01	14.74	85.26	
	62.50	0.22	0.21	0.24	0.22	0.01	24.94	75.06	
	31.25	0.39	0.33	0.32	0.34	0.02	39.00	61.00	
	15.62	0.78	0.79	0.81	0.80	0.01	90.25	9.75	
	7.81	0.87	0.89	0.87	0.88	0.01	99.32	0.68	

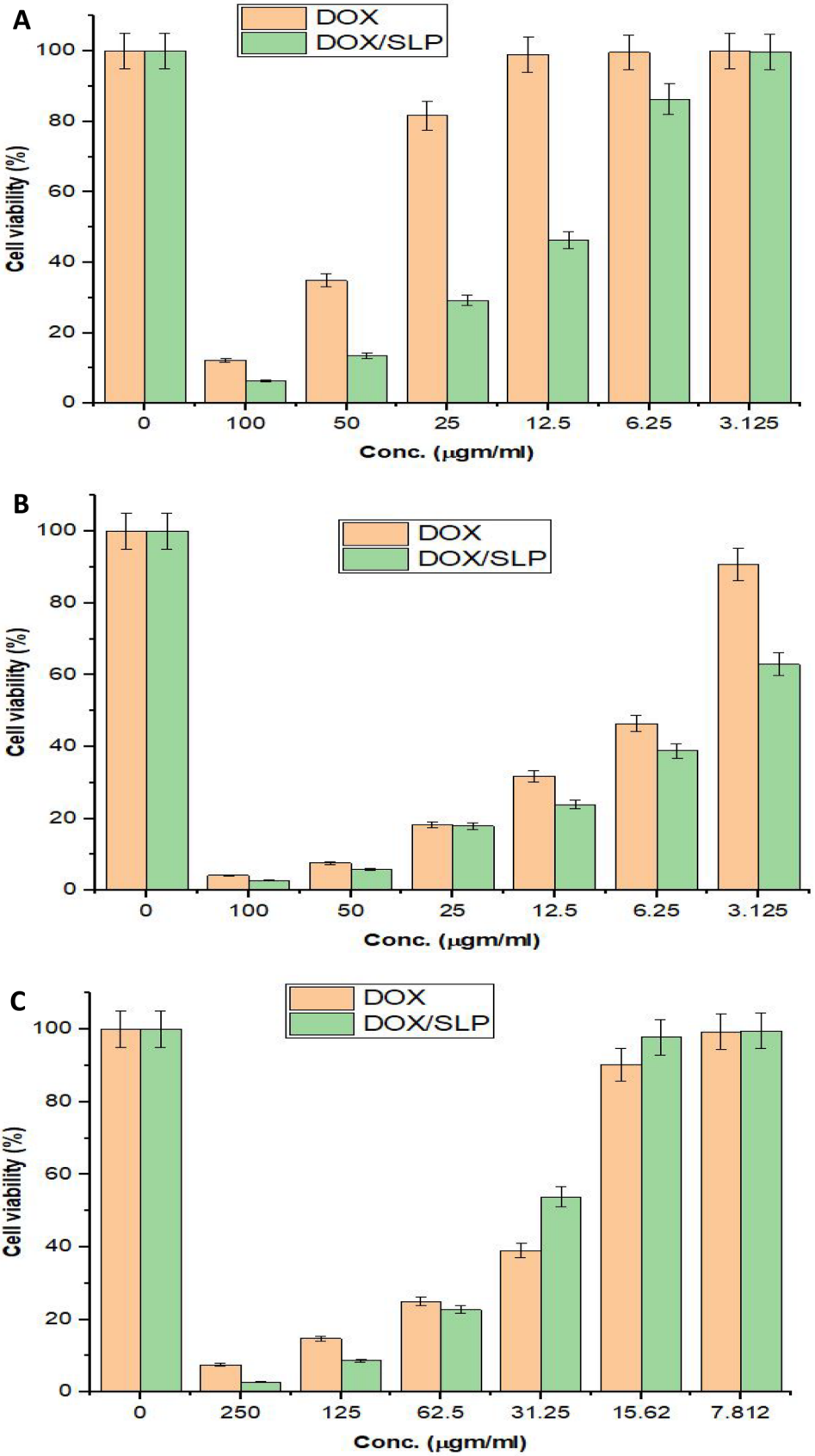

Fig. 7 Cell viability of **A** Vero as a normal cell exposed to 100, 50, 25, 12.5, 6.25, and 3.125 µg/ml, **B** Mcf-7 cells exposed to 100, 50, 25, 12.5, 6.25, and 3.125 µg/ml, and **C** Mcf-7 cells exposed to 250, 125, 62.5, 31.25, 15.62, and 7.812 µg/ml of DOX (orange line) and DOX/SLP (gray line) on all

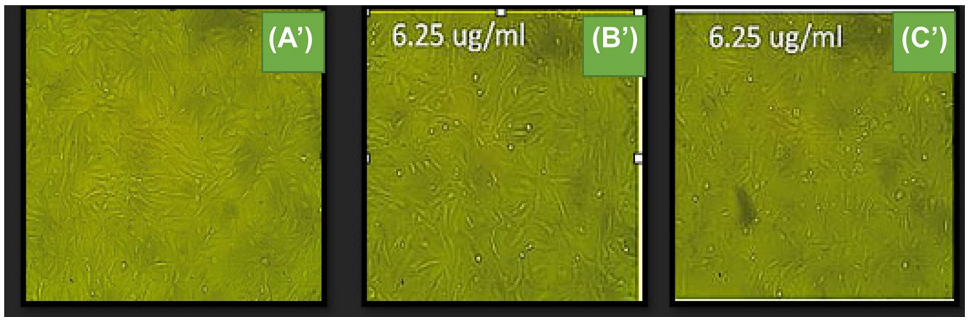

Fig. 8 Morphology of Vero cells: a control Vero (**A′**), the effect of free DOX with concentration (6.25 µg/ml) (**B′**), and the effect of DOX/SLP with concentration (6.25 µg/ml) (**C′**)

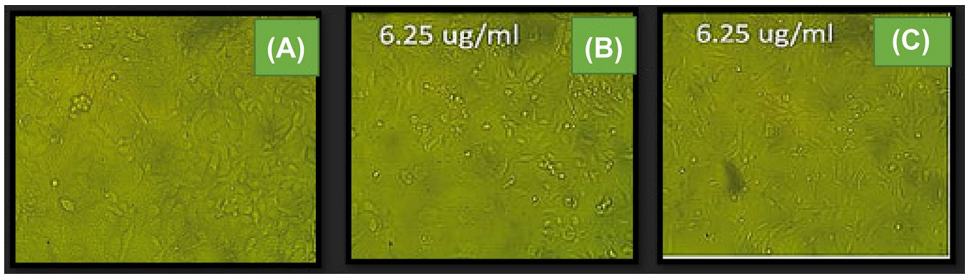

Fig. 9 Morphology of Mcf-7 cells at low conc.: a control Mcf-7 (**A**), the effect of free DOX with concentration (6.25 µg/ml) (**B**), and the effect of DOX/SLP with concentration (6.25 µg/ml) (**C**)

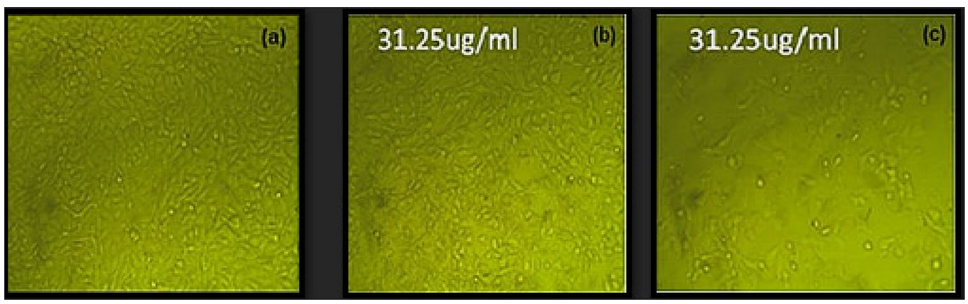

Fig. 10 Morphology of Mcf-7 cells at high conc.: a control Mcf-7 (**a**), the effect of free DOX with concentration (31.25 µg/ml) (**b**), and effect of DOX/SLP with concentration (31.25 µg/ml) (**c**)

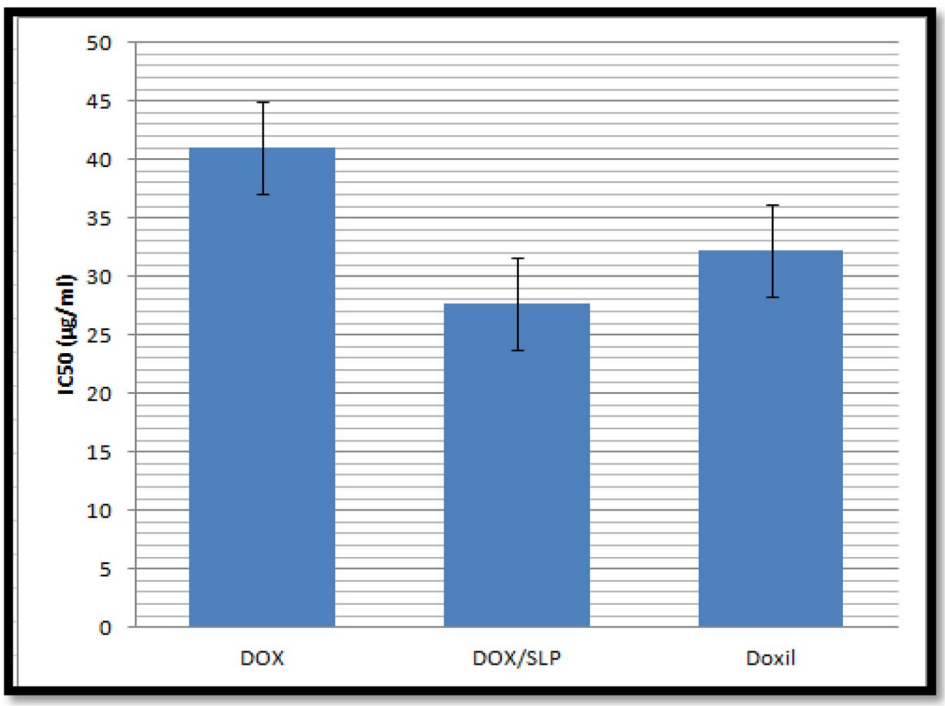

Fig. 11 The cytotoxicity as indicated by its IC_{50} of DOX, DOX/SLP, and Doxil

Conclusion

In this study, SLP extracted from soy lecithin (plant origin) was successfully synthesized for DOX delivery. DOX/SLP was used as a new drug conformation. The constructed sample is stable which will increase the circulation time of the drug carrier in the bloodstream. The optimal formulation of DOX/SLP exhibits a spherical shape (TEM images) with a size range (approximately 340 nm) and zeta potential (−22.3 mV) with high drug loading efficiency (83.675%) and transition temperature (47.4 °C). DOX was released from DOX/SLP in a controlled manner (up to 35 h). In addition, $IC_{50} \pm SD$ for DOX/SLP (27.72 ± 0.96 µg/ml) is smaller than that of free DOX and Doxil. In addition, DOX/SLP is considered a better candidate than other drug delivery systems from an economic point of view because soy lecithin is much cheaper than any other lipid. DOX/SLP is more effective in cancer treatment due to its biocompatibility. Thus the new conformation, DOX/SLP, is considered an excellent candidate for cancer treatment that can greatly decrease cancer treatment costs in addition to its great effect with low drug concentrations that will greatly reduce the side effects of chemotherapy.

Acknowledgements The authors wish to acknowledge the central labs in the National Research Center (NRC) and the Cancer Research Institute for their support during the experimental work.

Author Contribution 1st author: methodology, investigation, and writing original draft. 2nd author: conceptualization, supervision, and reviewing and editing. 3rd author: conceptualization, supervision, investigation, and reviewing and editing. 4th and corresponding author: conceptualization, methodology, investigation, supervision, writing and reviewing and editing.

Funding Open access funding provided by The Science, Technology & Innovation Funding Authority (STDF) in cooperation with The Egyptian Knowledge Bank (EKB).

Availability of Data and Materials All data are available from the corresponding author upon request.

Declarations

Ethics Approval and Consent to Participate Not applicable.

Consent for Publication All authors have read the submitted manuscript and consent for publication.

Competing Interests The authors declare no competing interests.

References

1. Samad A, Sultana Y, Aqil M. Liposomal drug delivery system: an update review. Curr Drug Deliv. 2007;4(4):297–305. https://doi.org/10.2174/156720107782151269.
2. Trucillo P, Campardelli R, Reverchon E. Liposomes: from bangham to supercritical fluids. Processes. 2020;8(9):1022. https://doi.org/10.3390/pr8091022.
3. Zhang J, Hu K, Di L, Wang P, Liu Z, Zhang J, Yue P, Song W, Zhang J, Chen T, Wang Z. Traditional herbal medicine and nanomedicine: converging disciplines to improve therapeutic efficacy and human health. Adv Drug Deliv Rev. 2021;(1);178:113964. https://doi.org/10.1016/j.addr.2021.113964
4. Lamichhane N, Udayakumar TS, D'Souza WD, Simone CB, Raghavan SR, Polf J, Mahmood J. Liposomes: clinical applications and potential for image-guided drug delivery. Molecules. 2018;23(2):288. https://doi.org/10.3390/molecules23020288.
5. Patil VV, Galge RV, Thorat BN. Extraction and purification of phosphatidylcholine from soyabean lecithin. Sep Purif Technol. 2010;75(2):138–44. https://doi.org/10.1016/j.seppur.2010.08.006.
6. Purwoko RY, Rosliana I, Purwaningsih EH, Freisleben HJ, Adiwinata J. Liposome formulation of soybean phosphatidylcholine extract from argomulyo variety soy to replace the toxicity of injectable phosphatidylcholine solution containing sodium deoxycholate. Int J Pharmtech Res. 2016;9(2):166–75.
7. Ahmad SS, Reinius MA, Hatcher HM, Ajithkumar T.V. Anticancer chemotherapy in teenagers and young adults: managing long term side effects. BMJ. 2016;354. https://doi.org/10.1136/bmj.i4567
8. Agunbiade TA, Zaghlol RY, Barac A. Heart failure in relation to anthracyclines and other chemotherapies. Methodist Debakey Cardiovasc J. 2019;15(4):243. https://doi.org/10.14797/mdcj-15-4-243.
9. Thron CF, Oshira C, Marsh S, Hernandez-Boussard T, McLeod H, Klein TE, Altman RB. Doxrubicin pathways: pharmacodynamics and advers effects. Pharmacogenet Genomics. 2011;21(7):440. https://doi.org/10.1097/FPC.0b013e32833ffb56.
10. Weiss RB. The anthracyclines: will we ever find a better doxorubicin?. In Seminars in Oncology. 1992;19(6):670–686. https://europepmc.org/article/med/1462166
11. Kowalczuk D, Piticha M. Application of FTIR method for the assessment of immobilization of active substances in the matrix of biomedical materials. Materials. 2019;12(18):2972. https://doi.org/10.3390/ma12182972.
12. Zhai B, Wu Q, Wang W, Zhang M, Han X, Li Q, Chen X, Huang X, Li G, Zhang Q. Preparation, characterization, pharmacokinetics and anticancer effects of PEGylated β-elemene liposomes. Cancer Biol Med. 2020;17(1):60. https://doi.org/10.20892/j.issn.2095-3941.2019.0156
13. Bozkurt O, Bayari SH, Servecan M, Krafft C, Popp J, Severcan F. Structural alternations in rat liver proteins due to streptozotocin-induced diabetes and the recovery effect of selenium: Fourier transform infrared microscopy and neural network study. J Biomed Opt. 2012;17(7):076023. https://doi.org/10.1117/1.JBO.17.7.076023
14. Le NT, Nguyen DT, Nguyen NH, Nguyen CK, Nguyen DH. Methoxy polyethylene glycol-cholesterol modified soy lecithin

liposomes for poorly water-soluble anticancer drug delivery. J Appl Polym Sci. 2012;138(7):49858. https://doi.org/10.1002/app.49858.
15. Korkmaz F, Severcan F. Effect of progesterone on DPPC membrane: evidence for lateral phase separation and inverse action in lipid dynamics. Arch Biochem Biophys. 2005;440(2):141–7. https://doi.org/10.1016/j.abb.2005.06.013.
16. Aguilar ZP. Chapter 5-targeted drug delivery. Nanomater Med Appl. 2013:181–234. https://doi.org/10.1016/B978-0-12-385089-8.00005-4
17. Liu B, Jin Z, Chen H, Liang L, Li Y, Wang G, Zhang J, Xu T. Electrospun poly (L-lactic acid)/gelatine membranes loaded with doxorubicin for effective suppression of glioblastoma cell growth in vitro and in vivo. Regen Biomater. 2021;8(5):1–12. https://doi.org/10.1093/rb/rbab043.
18. O'Neill SD, Leopold AC. An assessment of phase transition in soybean membranes. Plant Physiol. 1982;70(5):1405–9. https://doi.org/10.1104/pp.70.5.1405.
19. Kalepu S, Sunilkumar KT, Betha S, Mohanvarma M. Liposomal drug delivery system-a comprehensive review. Int J Drug Dev Res. 2013;5(4):62–75. https://doi.org/10.7324/JAPS.2022.120501.
20. Noshahr KD, Shamsi F, Valtchev P, Kokhaei P, Hemati M, Eidgahi MR, Khaleghian A. Optimization of post-insertion method to conjugate Doxil with anti-CD133 monoclonal antibodies: investigating the specific binding and cytotoxicity to colorectal cancer cells in vitro. Saudi Pharm J. 2020;28(11):1392–401. https://doi.org/10.1016/j.jsps.2020.09.003.
21. Vu MT, Le NT, Pham TL, Nguyen NH, Nguyen DH. Development and characterization of soy lecithin liposome as potential drug carrier systems for codelivery of letrozole and paclitaxel. J Nanomater. 2020;2020. https://doi.org/10.1155/2020/8896455
22. Huang Z, Li X, Zhang T, Song Y, She Z, Li J, Deng Y. Progress involving new techniques for liposome preparation. Asian J Pharm Sci. 2014;9(4):176–82. https://doi.org/10.1016/j.ajps.2014.06.001.
23. Mady MM, Darwish MM. Effect of chitosan coating on the characteristics of DPPC liposomes. J Adv Res. 2010;1(3):187–91. https://doi.org/10.1016/j.jare.2010.05.008.
24. Garcia-Diez R, et al. Size determination of a liposomal drug by small-angle X-ray scattering using continuous contrast variation. Langmuir. 2016;32:772–8. https://doi.org/10.1021/acs.langmuir.5b02261.
25. Lankalapalli S, Tenneti VS. Drug delivery through liposomes. Smart Drug Deliv. 2022;6:1–24.
26. Smith MC, Crist RM, Clogston JD. Zeta potential: a case study of cationic, anionic, and neutral liposomes. Anal Bioanal Chem. 2017;409:5779–87.
27. Le NT, Cao VD, Nguyen TN, Le TT, Tran TT, Hoang Thi TT. Soy lecithin-derived liposomal delivery systems: Surface modification and current applications. Int J Mol Sci. 2019;20(19):4706. https://doi.org/10.3390/ijms20194706.
28. Fesahat F, Khoshneviszadeh M, Foroumadi A, Vahidi A, Fereidounpour M, Sakhteman A. Cytotoxicity of some 1-(2, 4-dihydroxyphenyl)-3-(4-phenylpiperidin-1-yl) prop-2-en-1-one derivatives using MTT assay. Trends Pharmacol. 2015;1(1):20–4.
29. Gkionis L, Campbell RA, Aojula H, Harris LK, Tirella A. Manufacturing drug co-loaded liposomal formulations targeting breast cancer: influence of preparative method on liposomes characteristics and in vitro toxicity. Int J Pharm. 2020;590:119926. https://doi.org/10.1016/j.ijpharm.2020.119926
30. An WF, Tolliday N. Cell-based assays for high-throughput screening. Mol Biotechnol. 2010;45(2):180–6. https://doi.org/10.1007/s12033-010-9251-z.
31. Gewirtz D. A critical evaluation of the mechanisms of action proposed for the antitumor effects of the anthracycline antibiotics adriamycin and daunorubicin. Biochem Pharmacol. 1999;57(7):727–41. https://doi.org/10.1016/S0006-2952(98)00307-4.
32. Kautzka z, Clement S, Goldys EM, Deng W. Light-triggered liposomal cargo delivery platform incorporating photosensitizers and gold nanoparticles for enhanced singlet oxygen generation and increased cytotoxicity. Int J Nanomed. 2017;12:969. https://doi.org/10.2147/IJN.S126553
33. Laginha KM, Verwoert S, Charrois GJ, Allen TM. Determination of doxorubicin levels in whole tumor and tumor nuclei in murine breast cancer tumors. Clin Cancer Res. 2005;11(19):6944–9. https://doi.org/10.1158/1078-0432.CCR-05-0343.
34. Elbialy NS, Mady MM. Ehrlich tumor inhibition using doxorubicin containing liposomes. Saudi Pharm J. 2015;23(2):182–7. https://doi.org/10.1016/j.jsps.2014.07.003.
35. Molavi O, Xiong XB, Douglas D, Kneteman N, Nagata S, Pastan I, Chu Q, Lavasanifar A, Lai R. Anti-CD30 antibody conjugated liposomal doxorubicin with significantly improved therapeutic efficacy against anaplastic large cell lymphoma. Biomaterials. 2013;34(34):8718–25. https://doi.org/10.1016/j.biomaterials.2013.07.068.